CMS Physics Analysis Summary

Contact: cms-pag-conveners-heavyions@cern.ch 2019/05/21

Production of Λ_C^+ baryons in proton-proton and lead-lead collisions at $\sqrt{s_{NN}} = 5.02$ TeV

The CMS Collaboration

Abstract

The differential cross sections of Λ_C^+ baryon production are measured via the exclusive decay channel $\Lambda_C^+ \to pK^-\pi^+$, as a function of transverse momentum (p_T) in proton-proton (pp) and lead-lead (PbPb) collisions at a nucleon-nucleon center-of-mass energy of 5.02 TeV with the CMS detector at the LHC. The measurement is performed within the Λ_C^+ rapidity interval $|y| < 1.0$ in the p_T range of 5-20 GeV/c in pp and 10-20 GeV/c in PbPb collisions. The observed yields of Λ_C^+ for p_T of 10-20 GeV/c suggest a possible suppression in central PbPb collisions compared to pp collisions. The Λ_C^+/D^0 production ratio in pp collisions is compared to theoretical models. In PbPb collisions, this ratio is consistent with the result from pp collisions in their common p_T range.

1 Introduction

Measurements of heavy-quark production provide unique inputs in understanding the parton energy loss and the degree of thermalization in the quark-gluon plasma (QGP) [1] formed in high energy heavy ion collisions. Compared to light quarks, different mechanisms [2] are expected to dominate the interaction between heavy quarks and the medium. Besides the in-medium interactions, a detailed study of the hadronization process is critical for the interpretation of experimental data. In relativistic heavy ion collisions, in addition to the fragmentation process present in proton-proton (pp) collisions, hadron production can also occur via coalescence, where partons combine with each other while traversing the QGP medium [3]. For the production of hadrons with up, down, or strange quarks [4, 5], the significant enhancement of the baryon-to-meson ratio observed in heavy ion collisions and its dependence on centrality (i.e., the degree of overlap of the two colliding nuclei) can be interpreted as evidence of hadronization via coalescence. The nuclear modification factor R_{AA} is the ratio of the yield in heavy ion collisions to that in pp collisions scaled by the number of nucleon-nucleon (NN) interactions. In D^0 meson production, R_{AA} is observed to increase for p_{T} of about 0 GeV/c to 1.5 GeV/c and decrease from 2 GeV/c to 6 GeV/c in heavy ion collisions, an effect that can be reproduced by models involving coalescense [6]. The coalescence contribution to the baryons production is expected to be more significant than for mesons because of their larger number of constituent quarks. For example, models involving coalescence of charm and light-flavor quarks predict a large enhancement in the $\Lambda_{\mathrm{c}}^{+}/\mathrm{D}^0$ production ratio in heavy ion collisions relative to pp collisions and also predict that the enhancement has a strong p_{T} dependence [7–9]. Comparison of Λ_{c}^{+} baryon production in pp and lead-lead (PbPb) collisions can thus shed new light on understanding heavy-quark transport in the medium and heavy-quark hadronization via coalescence. All discussions of Λ_{c}^{+} and D^0 also include the corresponding charge conjugate states.

Recently, the production of Λ_{c}^{+} baryons for a variety of collision configurations has been measured in a similar p_{T} range by the LHC experiments ALICE and LHCb in the central and forward regions, respectively [10–13]. Both experiments measured the Λ_{c}^{+} p_{T}-differential cross sections in pp collisions at a center-of-mass energy of $\sqrt{s} = 7$ TeV and compared them to theoretical predictions using the next-to-leading order Generalized Mass Variable Flavor Number Scheme [14]. The LHCb results for the rapidity range $2.0 < y < 4.5$ were found to be compatible with theory [12], while the ALICE values for $|y| < 0.5$ were larger than the predictions [10]. The ALICE experiment also reported $\Lambda_{\mathrm{c}}^{+}/\mathrm{D}^0$ production ratios in 7 TeV pp collisions, as well as in proton-lead (pPb) and PbPb collisions at an NN center-of-mass energy of $\sqrt{s_{\mathrm{NN}}} = 5.02$ TeV. The ALICE ratios from pp and pPb collisions [10] were found to be above the corresponding LHCb values [12, 13] (however in different rapidity ranges), with the latter agreeing with theoretical predictions. The ALICE $\Lambda_{\mathrm{c}}^{+}/\mathrm{D}^0$ production ratio for $6 < p_{\mathrm{T}} < 12$ GeV/c in PbPb collisions was measured to be larger than in pp and pPb collisions, and this difference can be described using a model involving only coalescence in hadronization [11]. The ALICE measurements of the R_{AA} of Λ_{c}^{+} baryons in pPb and PbPb collisions were found to be compatible, with unity and less than unity, respectively, but do little to constrain models owing to large uncertainties [10, 11].

In this note, we report on the first measurements of Λ_{c}^{+} baryon production in pp and PbPb collisions at high p_{T}. The data were collected at $\sqrt{s_{\mathrm{NN}}} = 5.02$ TeV in 2015 using the CMS detector. The Λ_{c}^{+} baryons are reconstructed in the central region ($|y| < 1$) via the hadronic decay channel $\Lambda_{\mathrm{c}}^{+} \to \mathrm{pK}^{-}\pi^{+}$. The differential cross section, as well as the $\Lambda_{\mathrm{c}}^{+}/\mathrm{D}^0$ production ratio, are measured in the p_{T} ranges 5–20 and 10–20 GeV/c in pp and PbPb collisions, respectively. The $\Lambda_{\mathrm{c}}^{+}/\mathrm{D}^0$ production ratios use the corresponding CMS measurements of D^0 production [15].

Centrality bins for PbPb collisions are given in percentage ranges of the total inelastic hadronic cross section, with the 0–30% centrality bin corresponding to the 30% of collisions having the largest overlap of the two nuclei. The values of R_{AA} are obtained for three centrality intervals: 0–100%, 0–30%, and 30–100%.

2 The CMS detector

The central feature of the CMS apparatus is a superconducting solenoid of 6 m internal diameter, providing a magnetic field of 3.8 T. Within the solenoid volume are a silicon tracker, a lead tungstate crystal electromagnetic calorimeter, and a brass and scintillator hadron calorimeter, each composed of a barrel and two endcap sections. The tracker measures charged particles within the pseudorapidity range $|\eta| < 2.5$ and the calorimeters record deposited energy for particles with $|\eta| < 3.0$. Two forward hadron (HF) calorimeters use steel as an absorber and quartz fibers as the sensitive material. The two HF calorimeters are located 11.2 m from the interaction region, one on each end, and together they extend the calorimeter coverage from $|\eta| = 3.0$ to 5.2. Each HF calorimeter consists of 432 readout towers, containing long and short quartz fibers running parallel to the beam, providing information on the shower energy and the relative contribution originating from hadrons versus electrons and photons. A detailed description of the CMS experiment can be found in Ref. [16].

3 Event reconstruction and simulated samples

The collision centrality is determined from the total transverse energy deposited in both HF calorimeters and was utilized by the two triggers used in this analysis [17]. One trigger selected minimum-bias (MB) events by requiring energy deposits in both HF calorimeters above approximately 1 GeV. As not all MB events could be saved, an additional trigger selected the more peripheral centrality region of 30–100% for PbPb events. The integrated luminosities of pp collisions, PbPb collisions with centrality 0–100%, and PbPb collisions with centrality 30–100% are $38\,\mathrm{nb}^{-1}$, $44\,\mu\mathrm{b}^{-1}$, and $102\,\mu\mathrm{b}^{-1}$, respectively.

The track reconstruction algorithms used in this study for pp and PbPb collisions are described in Refs. [18] and [19], respectively. In PbPb collisions, minor modifications are made to the pp reconstruction algorithm in order to accommodate the much larger track multiplicities. Tracks are required to have a relative p_{T} uncertainty of less than 30% in PbPb collisions and 10% in pp collisions. In PbPb collisions, tracks must also have at least 11 hits and satisfy a stringent fit quality requirement, specifically that the χ^2 per degree of freedom be less than 0.15 times the number of tracker layers with a hit.

For the offline analysis, events must pass selection criteria designed to reject events from background processes (beam-gas interactions and nonhadronic collisions), as described in Ref. [19]. Events are required to have at least one reconstructed primary interaction vertex [20] with a distance from the center of the nominal interaction region of less than 15 cm along the beam axis. In addition, in PbPb collisions, the shapes of the clusters in the pixel detector have to be compatible with those expected from particles produced at the primary vertex location [21]. The PbPb collision events are also required to have at least three towers in each HF detector with energy deposits of more than 3 GeV per tower. These criteria select $(99 \pm 2)\%$ of inelastic hadronic PbPb collisions. Selection efficiencies higher than 100% reflect the possible presence of ultra-peripheral (nonhadronic) collisions in the selected event sample.

Monte Carlo (MC) simulated event samples are used to optimize the selection criteria, calculate

the acceptance times efficiency, and estimate the systematic uncertainties. The MC samples contain 4 sub-channels: $\Lambda_c^+ \to p\overline{K}^*(892)^0 \to pK^-\pi^+$, $\Lambda_c^+ \to \Delta(1232)^{++}K^- \to pK^-\pi^+$, $\Lambda_c^+ \to \Lambda(1520)\pi^+ \to pK^-\pi^+$, and $\Lambda_c^+ \to pK^-\pi^+$ (nonresonant), with no modeling of interference between the sub-channels. Proton-proton collisions are generated with PYTHIA8.212 [22] tune CUETP8M1 [23], hereafter referred to as PYTHIA8. For the PbPb MC samples, each PYTHIA8 event containing a Λ_c^+ baryon is embedded into a PbPb collision event generated with HYDJET 1.8 [24], which is tuned to reproduce global event properties such as the charged-hadron p_T spectrum and particle multiplicity. The Λ_c^+ is decayed with EVTGEN 1.3.0 [25] and all particles are propagated through the CMS detector using the GEANT4 package [26].

4 Signal extraction

The $\Lambda_c^+ \to pK^-\pi^+$ candidates are reconstructed by selecting three charged tracks with $|\eta| < 1.2$ and a net charge of $+1$. All tracks must have $p_T > 0.7\,(1.0)$ GeV/c for pp (PbPb) events. During the invariant mass reconstruction, both possibilities for the mass assignments of the same-sign tracks are considered, while the kaon mass is assigned to the opposite-signed track. The incorrect assignment results in a broad distribution in the invariant mass (about 30 times the signal width) and is indistinguishable from the combinatorial background.

As the event multiplicities for pp and PbPb collisions are substantially different, the selection criteria were optimized separately. In the optimization, simulated events in which a reconstructed Λ_c^+ candidate is matched to a generated Λ_c^+ baryon are used as the signal sample, and data events from the mass sideband region are used as the background sample. Requirements are made on three topological and three kinematic variables. The three topological criteria are: the χ^2 probability of the vertex fit to the three charged tracks making up the Λ_c^+ candidate, the angle between the Λ_c^+ candidate momentum and the vector connecting the production and decay vertices in radians (α), and the separation between the two vertices. While more than one collision per bunch crossing is rare in PbPb collisions, it is common in pp collisions. Therefore, two-dimensional variables in the transverse plane with respect to the beamline are used for α and decay length in pp collisions, while three-dimensional variables with respect to the primary vertex are used for PbPb collisions. For the PbPb events, the topological requirements are χ^2 probability above 20%, $\alpha < 0.1$, and decay length greater than 3.75σ, where σ is the uncertainty on the separation. For pp events, the corresponding requirements are χ^2 probability above 8%, $\alpha < 0.4$, and decay length greater than 2.25σ. The kinematic requirements are kaon (proton) p_T divided by the Λ_c^+ candidate p_T greater than 0.14 (0.28) for all events and pion p_T divided by the Λ_c^+ candidate p_T greater than 0.12 for PbPb events.

The Λ_c^+ baryon yields in each p_T interval are obtained from unbinned maximum likelihood fits to the invariant mass distribution in the range of 2.11–2.45 GeV/c^2. The signal shape is modeled by the sum of two Gaussian functions with the same mean, but different widths that are fixed on the basis of the simulated signal sample. One fit parameter scales both widths to accommodate a potential difference in the mass resolution between simulation and data, with the exception of the lowest p_T region (5–6 GeV/c) in the pp data, where this parameter was found to cause a bias in the fit and was fixed to the value that returned the smallest bias. The background is modeled with a third-order Chebyshev polynomial. Representative invariant mass distributions in pp and PbPb collisions are shown in Fig. 1.

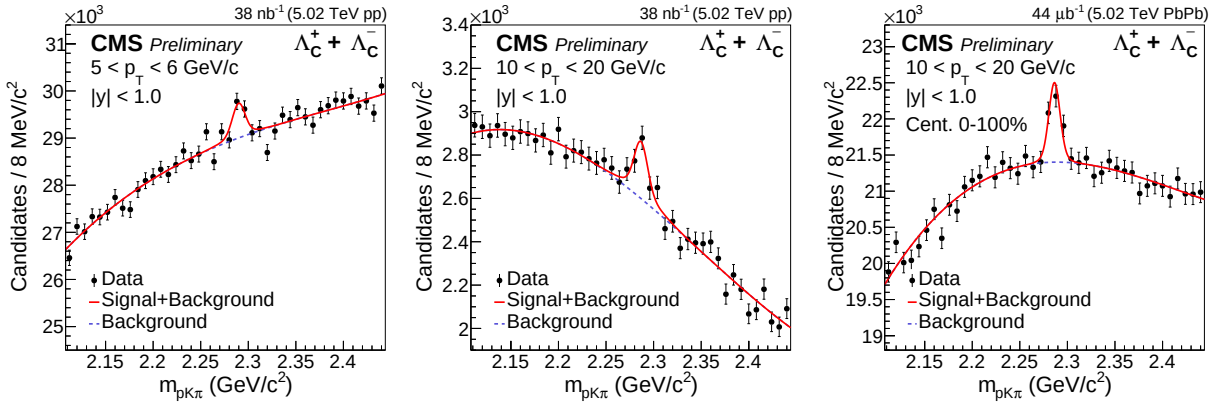

Figure 1: Invariant mass distribution of Λ_c^+ candidates with p_T = 5–6 GeV/c (left), 10–20 GeV/c (middle) in pp collisions, and p_T = 10–20 GeV/c in PbPb collisions within the centrality range 0–100% (right). The solid line represents the full fit and the dashed line represents the background component.

The Λ_c^+ baryon differential cross section in pp collisions is defined as:

$$\left.\frac{d\sigma_{pp}^{\Lambda_c^+}}{dp_T}\right|_{|y|<1.0} = \frac{1}{2\mathcal{L}\Delta p_T \mathcal{B}} \frac{N_{pp}^{\Lambda_c^+}|_{|y|<1.0}}{A\epsilon}, \tag{1}$$

where $N_{pp}^{\Lambda_c^+}|_{|y|<1.0}$ is the Λ_c^+ yield extracted in each p_T bin, $\mathcal{L}$ is the integrated luminosity, Δp_T is the width of each p_T bin, $\mathcal{B}$ is the branching fraction of the decay, and $A\epsilon$ is the product of the acceptance and efficiency. The factor of $\frac{1}{2}$ accounts for averaging the particle and antiparticle contributions. The Λ_c^+ differential cross section in PbPb collisions is defined as:

$$\frac{1}{\langle T_{AA}\rangle}\left.\frac{dN_{PbPb}^{\Lambda_c^+}}{dp_T}\right|_{|y|<1.0} = \frac{1}{\langle T_{AA}\rangle}\frac{1}{2N_{events}\Delta p_T \mathcal{B}} \frac{N_{PbPb}^{\Lambda_c^+}|_{|y|<1.0}}{A\epsilon}, \tag{2}$$

where N_{events} is the number of MB events used for the analysis and $\langle T_{AA}\rangle$ is the nuclear overlap function, which is equal to the average number of NN binary collisions ($\langle N_{coll}\rangle$) divided by the NN inelastic cross section, and can be interpreted as the NN-equivalent integrated luminosity per heavy ion collision. The values of $\langle T_{AA}\rangle$, $\langle N_{coll}\rangle$, and the average number of participating nucleons ($\langle N_{part}\rangle$), calculated by a Monte Carlo Glauber model [27], in which the NN inelastic cross section (70 mb) is used as an input parameter, are the averages of these quantities over the events in the given centrality range, and are listed in Table 1.

Table 1: Summary of the $\langle N_{coll}\rangle$, $\langle T_{AA}\rangle$, and $\langle N_{part}\rangle$ values for three PbPb centrality ranges.

Centrality	$\langle T_{AA}\rangle$ [mb^{-1}]	$\langle N_{part}\rangle$	$\langle N_{coll}\rangle$
0–30%	$15.41^{+0.33}_{-0.47}$	$270.7^{+3.2}_{-3.4}$	1079^{+74}_{-78}
30–100%	$1.41^{+0.09}_{-0.06}$	$46.8^{+2.4}_{-1.2}$	98^{+8}_{-6}
0–100%	$5.61^{+0.16}_{-0.19}$	$114.0^{+2.6}_{-2.6}$	393^{+26}_{-28}

The nuclear modification factor R_{AA} is computed as:

$$R_{AA}(p_T) = \frac{1}{\langle T_{AA}\rangle}\frac{dN_{PbPb}^{\Lambda_c^+}}{dp_T} \Big/ \frac{d\sigma_{pp}^{\Lambda_c^+}}{dp_T}. \tag{3}$$

The values of $A\epsilon$ are obtained from MC simulation as a fraction in which the denominator is all Λ_c^+ baryons with $|y| < 1$ and the numerator is all reconstructed Λ_c^+ candidates that pass the selection criteria and are matched to a generated Λ_c^+ baryon. The p_T spectrum of the generated events is weighted to match the observed data for the pp sample. As the PbPb results are given for just one p_T range, an alternative method is used to correct the p_T spectra in simulation. Under the transverse mass scaling hypothesis (m_T scaling) [28], the Λ_c^+ baryon p_T spectrum is obtained for the 0–100% centrality region from the D^0 measurements [15] using the function $m^2(\Lambda_c^+) + p_T^2(\Lambda_c^+) = m^2(D^0) + p_T^2(D^0)$. For the PbPb data set, the centrality distribution in simulation is also reweighted to match the data. The values of $A\epsilon$ vary from 7 to 19% between the lowest and highest p_T bins in pp collisions, and are 4–5% for the three centrality bins in PbPb collisions.

5 Systematic uncertainties

Systematic uncertainties arise from estimating the signal yield, the ability of the MC simulation to reproduce the combined acceptance and efficiency, the branching fraction of the decay mode, and the integrated luminosity. Unless otherwise indicated, the total systematic uncertainty is obtained by adding the individual contributions in quadrature.

The systematic uncertainty in the signal yields is obtained by varying the modeling functions that are used for the signal and background contributions. The background function is changed from the default third- to second- and fourth-order Chebyshev polynomials, with the maximum difference in yield between these two alternative functions and the default fit function taken as the systematic uncertainty. This amounts to 4–10% and 7–9% for pp and PbPb collisions, respectively. The default signal model function is the sum of two Gaussian functions. For the pp collision data, the alternative model is a single Gaussian function. For the PbPb collision data, two alternative models are tried, a single Gaussian function and the sum of two Gaussian functions with the shape parameters fixed to the values found in the $10 < p_T < 20\,\text{GeV}/c$ bin of the pp collision data. As the signal width is fixed for events with Λ_c^+ $p_T < 6\,\text{GeV}/c$, an additional systematic uncertainty is assessed by varying the width by $\pm 40\%$, corresponding to the typical variations observed in other p_T bins in pp and PbPb collisions. The uncertainty due to the modeling of the signal is 10–32% for pp collisions and 6–13% for PbPb collisions, and is largest at low p_T (pp) and in peripheral events (PbPb).

Four systematic uncertainties associated with the MC modeling of the data are evaluated. The first uncertainty measures the effect of the selection criteria variation. We define a double ratio as:

$$\mathcal{DR} = \frac{N_{\text{Data}}(\text{varied})}{N_{\text{Data}}(\text{nominal})} \Big/ \frac{N_{\text{MC}}(\text{varied})}{N_{\text{MC}}(\text{nominal})}\,, \tag{4}$$

where N_{Data}(nominal) and N_{Data}(varied) are the yields obtained from data using the default and alternative selection criteria, respectively, and N_{MC}(nominal) and N_{MC}(varied) are the corresponding yields from the simulated events. For each of the topological selection criteria, the double ratio is evaluated at many different values of the selection criterion. The specific ranges for pp collision events are $>1.5\sigma$ to $>6\sigma$, $>5\%$ to $>45\%$, and <0.1 to no cut for decay length, vertex fit probability, and α, respectively. The corresponding ranges for PbPb collision events are $>2.5\sigma$ to $>8\sigma$, $>5\%$ to $>45\%$, and <0.05 to <0.2. For all but the α cut in PbPb collisions, $\mathcal{DR}$ is plotted as a function of the selection value and fit to a linear function. The systematic uncertainty is taken as the difference between unity and the value of the fitted line at the point where no selection is applied. For the α requirement in PbPb collisions, the systematic uncertainty is obtained from the biggest differences between unity and the value of $\mathcal{DR}$ from all of

the alternative selection values. Combining the results of the three topological selection criteria systematic uncertainties in quadrature results in uncertainties of 6% for the pp data set and 19% for the PbPb data sets. The second uncertainty arises from a potential mismodeling of the p_{T} distribution of Λ_{c}^{+} baryons because $A\epsilon$ is strongly dependent on the Λ_{c}^{+} p_{T}. In pp collisions, the default p_{T} shape is derived from the data. The spectrum from PYTHIA8 and a model calculation from Ref. [29] are used as alternative descriptions, with the maximum difference in $A\epsilon$ with respect to the nominal value taken as the systematic uncertainty. For PbPb collisions, the default p_{T} shape is obtained from m_{T} scaling of the measured D^0 p_{T} spectrum. An alternative p_{T} spectrum is obtained from PYTHIA8 and the difference in $A\epsilon$ is used as the systematic uncertainty, which amounts to 0–10% for pp collisions and 3–4% for PbPb collisions. The third uncertainty arises from imprecise knowledge of the resonant substructure of the $\mathrm{pK}^{-}\pi^{+}$ decay mode [30]. The calculation of $A\epsilon$ uses the appropriately weighted sum of the four known subchannels and the systematic uncertainty associated with this is evaluated by determining $A\epsilon$ for each sub-channel and adjusting the weights by the uncertainties of each branching fraction. The systematic uncertainty is obtained from the standard deviation of a Gaussian fit to the $A\epsilon$ values and is 8% for both pp and PbPb events. The fourth uncertainty associated with the MC modeling of the data is the track reconstruction efficiency, which is 4% for pp collisions [15] and 5% for PbPb collisions [31]. As there are three tracks in the Λ_{c}^{+} decay, the corresponding uncertainties on the measured p_{T} spectra are 12 and 15% for pp and PbPb, respectively, while for the $\Lambda_{\mathrm{c}}^{+}/\mathrm{D}^0$ production ratio, the uncertainties are 4 and 5%, respectively. For R_{AA}, the track reconstruction efficiency uncertainty is 19%, obtained by assuming the pp and PbPb uncertainties are independent and summing them in quadrature.

The overall $\Lambda_{\mathrm{c}}^{+} \to \mathrm{pK}^{-}\pi^{+}$ branching fraction uncertainty is 5.3% [30]. However, this effect is canceled when evaluating the systematic uncertainty of R_{AA}. The uncertainties of the integrated luminosity in pp collisions and the MB selection efficiency in PbPb collisions are 2.3% [32] and 2.0% [19], respectively. In calculating the $\Lambda_{\mathrm{c}}^{+}/\mathrm{D}^0$ production ratio, the uncertainties associated with D^0 from the yield extraction, selection criteria efficiency, and p_{T} shape are obtained from Ref. [15], while the uncertainties in the integrated luminosity in pp collisions and the MB selection efficiency in PbPb collisions cancel.

6 Results and discussion

Figure 2 shows the p_{T}-differential cross section of Λ_{c}^{+} baryon production in pp collisions for the range of $5 < p_{\mathrm{T}} < 20\,\mathrm{GeV}/c$ and in PbPb collisions for the range of $10 < p_{\mathrm{T}} < 20\,\mathrm{GeV}/c$, for three centrality classes. The 5.8% normalization uncertainty in the pp differential cross section arising from the integrated luminosity and branching fraction is not included in the boxes representing the systematic uncertainties for each data point. The corresponding normalization uncertainty in the PbPb results is included in the systematic uncertainty boxes for each data point. The shape of the p_{T} distribution in pp collisions is consistent with the PYTHIA8 calculation. While the data are systematically higher than PYTHIA8, the difference is not significant taking into account the uncertainty in the measurement.

The nuclear modification factor R_{AA} for Λ_{c}^{+} baryons in the p_{T} range 10–20 GeV/c is shown in Fig. 3 as a function of the number of participating nucleons $\langle N_{\mathrm{part}} \rangle$ for PbPb collisions. There is a hint that the production of Λ_{c}^{+} is suppressed in PbPb collisions for $p_{\mathrm{T}} > 10\,\mathrm{GeV}/c$, but no conclusion can be drawn due to the large uncertainty in the pp differential cross section. However, the ratio of the R_{AA} values for the 0–30% and 30–100% centrality ranges (which is independent of the pp uncertainty) shows evidence for more suppression in the more central PbPb collisions.

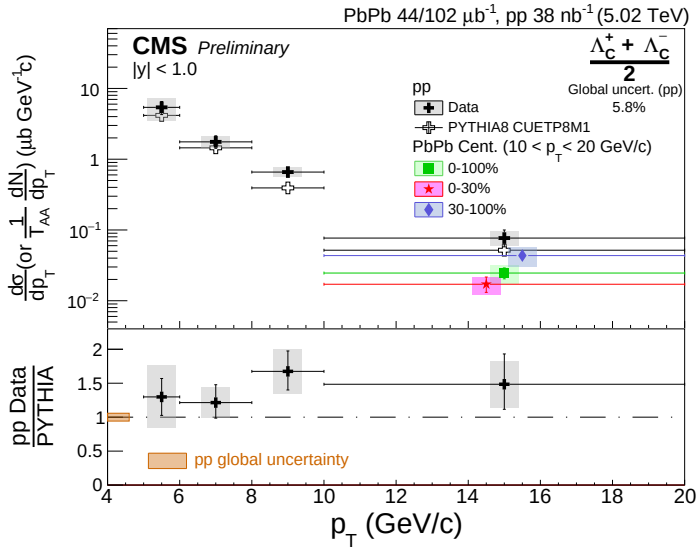

Figure 2: The p_{T}-differential cross sections for Λ_{c}^{+} baryon in pp collisions and in three centrality regions of PbPb collisions, along with the PYTHIA8 calculation for pp collisions. The boxes and error bars represent the systematic and statistical uncertainties, respectively. The PbPb data points are shifted in the horizontal axis for clarity. The lower panel shows the ratio of the measured p_{T}-differential cross section in pp data to the PYTHIA8 calculation. The box at unity in the lower panel indicates the 5.8% normalization uncertainty for pp collision arising from the integrated luminosity and branching fraction. The PbPb normalization uncertainty is included in the systematic uncertainty for each point.

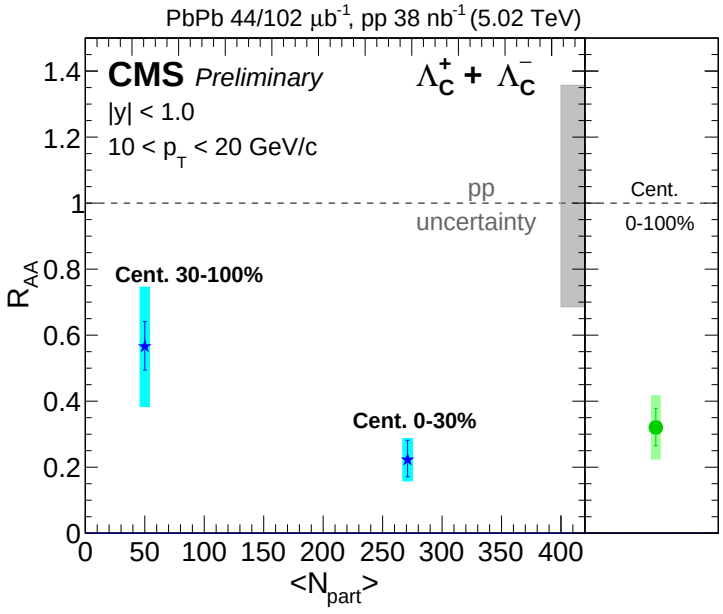

Figure 3: The nuclear modification factor R_{AA} versus $\langle N_{\mathrm{part}} \rangle$. The boxes and error bars on the data points represent the systematic and statistical uncertainties in the numerator of Eq. (3), respectively. The box at unity indicates the total uncertainty in the pp differential cross section, which is common to all three R_{AA} values.

Figure 4 shows the Λ_c^+/D^0 production ratio as a function of p_T for pp collisions and PbPb collisions in the centrality range 0–100%. Because the uncertainties in the measured cross sections are asymmetric, the Λ_c^+/D^0 production ratio is obtained via a fit to the Λ_c^+ baryon mass spectrum with the Λ_c^+/D^0 production ratio as a free parameter and the statistical uncertainty of the D^0 yields included as a nuisance parameter. The production ratio found from pp collisions is similar in shape versus p_T but about three times larger in magnitude compared to the calculation from PYTHIA8.212 tune CUETP8M1. Results using the Monash 2013 [33] tune are found to be consistent with those from the CUETP8M1 tune. The hadronization in PYTHIA8.212 can be modified by adding a color reconnection (CR) mechanism in which the final partons in the string fragmentation are considered to be color connected in such a way that the total string length becomes as short as possible [34]. Figure. 4 shows that calculations using the "standard" color reconnection model are consistent with our results for the Λ_c^+/D^0 production ratio in pp collisions.

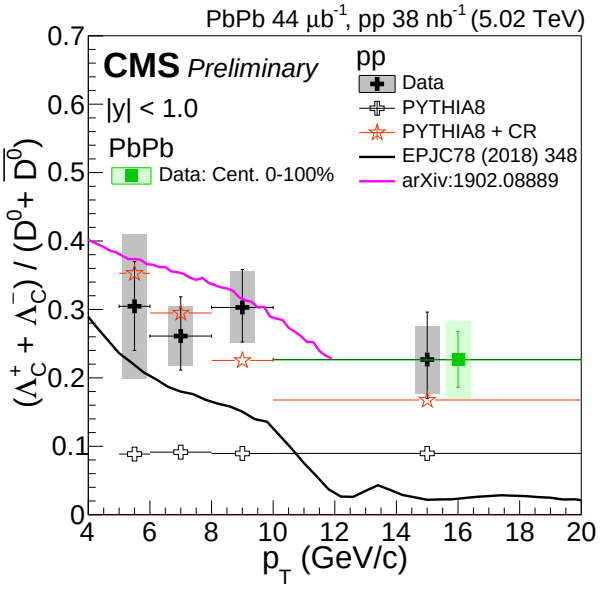

Figure 4: The Λ_c^+/D^0 production cross section ratio versus p_T from pp collisions as well as 0–100% centrality PbPb collisions. The boxes and error bars represent the systematic and statistical uncertainties, respectively. The PbPb data point is shifted in the horizontal axis for clarity. The open crosses and open stars represent the predictions of PYTHIA8 with the CUETP8M1 tune and with color reconnection [34], respectively. The black and pink lines are the calculations from Ref. [29] and Ref. [35], respectively. All predictions are for pp collisions.

The observation of a higher Λ_c^+/D^0 production ratio in data may suggest the need to introduce coalescence production in charm quark hadronization in pp collisions. Calculations using a model that includes both coalescence and fragmentation in pp collisions [29] are shown in Fig. 4 by the black line. Compared to the data, the model predicts a stronger dependence on p_T and underestimates the measurements for p_T above 10 GeV/c. Another recent model attempts to explain the large Λ_c^+/D^0 production ratio as arising from Λ_c^+ baryons that are produced from the decay of excited charm baryon states not included in the PYTHIA8 hadronization [35]. The prediction of this model, also shown in Fig. 4 by the pink line, provides a reasonable description of the data in the range where it is available.

In contrast to the ALICE observation of a large enhancement in the Λ_c^+/D^0 production ratio in the p_T range of 6–12 GeV/c for PbPb [11] compared to pp collisions [10], the CMS PbPb

measurement in the p_T range 10–20 GeV/c is consistent with the pp result. This lack of an enhancement may suggest that there is no significant contribution from the coalescence process for $p_T > 10$ GeV/c in PbPb collisions.

7 Summary

The p_T-differential cross sections of Λ_c^+ baryons have been measured in pp and PbPb collisions at a nucleon-nucleon center-of-mass energy of 5.02 TeV. The shape of the p_T distribution in pp collisions is well described by the PYTHIA8 event generator. A hint of suppression of Λ_c^+ production for $10 < p_T < 20$ GeV/c is observed in PbPb when compared to pp data, with central PbPb events showing stronger suppression. This possible suppression may originate from the strong interaction between the charm quark and the quark-gluon plasma medium, as previously indicated by the D^0 meson measurements. The Λ_c^+/D^0 production ratios in pp collisions are consistent with a model obtained by adding color reconnection in hadronization to PYTHIA8, and also with a model that includes enhanced contributions from the decay of excited charm baryons. A model including coalescence underpredicts the data for p_T above about 8-10 GeV/c. The Λ_c^+/D^0 production ratios in pp and PbPb collisions for p_T = 10–20 GeV/c are found to be consistent with each other. These two observations may suggest that the coalescence process does not play a significant role in Λ_c^+ baryon production in this p_T range.

References

[1] E. V. Shuryak, "Theory of Hadronic Plasma", *Sov. Phys. JETP* **47** (1978) 212. [Zh. Eksp. Teor. Fiz. **74** (1978) 408].

[2] A. Beraudo et al., "Extraction of Heavy-Flavor Transport Coefficients in QCD matter", *Nucl. Phys. A* **979** (2018) 21, doi:10.1016/j.nuclphysa.2018.09.002, arXiv:1803.03824.

[3] V. Greco, C. M. Ko, and P. Lévai, "Parton Coalescence and the Antiproton/Pion Anomaly at RHIC", *Phys. Rev. Lett.* **90** (2003) 202302, doi:10.1103/PhysRevLett.90.202302, arXiv:nucl-th/0301093.

[4] STAR Collaboration, "Identified baryon and meson distributions at large transverse momenta from Au+Au collisions at $\sqrt{s_{NN}}$ = 200 GeV", *Phys. Rev. Lett.* **97** (2006) 152301, doi:10.1103/PhysRevLett.97.152301, arXiv:nucl-ex/0606003.

[5] STAR Collaboration, "Systematic Measurements of Identified Particle Spectra in pp, d+Au and Au+Au Collisions from STAR", *Phys. Rev. C* **79** (2009) 034909, doi:10.1103/PhysRevC.79.034909, arXiv:0808.2041.

[6] STAR Collaboration, "Observation of D^0 meson nuclear modifications in Au+Au collisions at $\sqrt{s_{NN}}$ = 200 GeV", *Phys. Rev. Lett.* **113** (2014) 142301, doi:10.1103/PhysRevLett.113.142301, arXiv:1404.6185.

[7] Y. Oh, C. M. Ko, S. H. Lee, and S. Yasui, "Heavy baryon/meson ratios in relativistic heavy ion collisions", *Phys. Rev. C* **79** (2009) 044905, doi:10.1103/PhysRevC.79.044905, arXiv:0901.1382.

[8] S. H. Lee et al., "Λ_c enhancement from strongly coupled quark-gluon plasma", *Phys. Rev. Lett.* **100** (2008) 222301, doi:10.1103/PhysRevLett.100.222301, arXiv:0709.3637.

[9] S. Ghosh et al., "Diffusion of Λ_c in hot hadronic medium and its impact on Λ_c/D ratio", *Phys. Rev. D* **90** (2014) 054018, doi:10.1103/PhysRevD.90.054018, arXiv:1407.5069.

[10] ALICE Collaboration, "Λ_c^+ production in pp collisions at $\sqrt{s} = 7$ TeV and in p-Pb collisions at $\sqrt{s_{\rm NN}} = 5.02$ TeV", *JHEP* **04** (2018) 108, doi:10.1007/JHEP04(2018)108, arXiv:1712.09581.

[11] ALICE Collaboration, "Λ_c^+ production in Pb-Pb collisions at $\sqrt{s_{\rm NN}} = 5.02$ TeV", *Submitted to: Phys. Lett. B* (2018) arXiv:1809.10922.

[12] LHCb Collaboration, "Prompt charm production in pp collisions at $\sqrt{s} = 7$ TeV", *Nucl. Phys. B* **871** (2013) 1, doi:10.1016/j.nuclphysb.2013.02.010, arXiv:1302.2864.

[13] LHCb Collaboration, "Prompt Λ_c^+ production in pPb collisions at $\sqrt{s_{\rm NN}} = 5.02$ TeV", *JHEP* **02** (2019) 102, doi:10.1007/JHEP02(2019)102, arXiv:1809.01404.

[14] M. A. G. Aivazis, J. C. Collins, F. I. Olness, and W.-K. Tung, "Leptoproduction of heavy quarks. II. A unified QCD formulation of charged and neutral current processes from fixed-target to collider energies", *Phys. Rev. D* **50** (1994) 3102, doi:10.1103/PhysRevD.50.3102.

[15] CMS Collaboration, "Nuclear modification factor of D^0 mesons in PbPb collisions at $\sqrt{s_{\rm NN}} = 5.02$ TeV", *Phys. Lett. B* **782** (2018) 474, doi:10.1016/j.physletb.2018.05.074, arXiv:1708.04962.

[16] CMS Collaboration, "The CMS experiment at the CERN LHC", *JINST* **3** (2008) S08004, doi:10.1088/1748-0221/3/08/S08004.

[17] CMS Collaboration, "Observation and studies of jet quenching in PbPb collisions at nucleon-nucleon center-of-mass energy = 2.76 TeV", *Phys. Rev.* **C84** (2011) 024906, doi:10.1103/PhysRevC.84.024906, arXiv:1102.1957.

[18] CMS Collaboration, "Description and performance of track and primary-vertex reconstruction with the CMS tracker", *JINST* **9** (2014) P10009, doi:10.1088/1748-0221/9/10/P10009, arXiv:1405.6569.

[19] CMS Collaboration, "Charged-particle nuclear modification factors in PbPb and pPb collisions at $\sqrt{s_{\rm NN}} = 5.02$ TeV", *JHEP* **04** (2017) 039, doi:10.1007/JHEP04(2017)039, arXiv:1611.01664.

[20] CMS Collaboration, "Description and performance of track and primary-vertex reconstruction with the CMS tracker", *JINST* **9** (2014) P10009, doi:10.1088/1748-0221/9/10/P10009, arXiv:1405.6569.

[21] CMS Collaboration, "Transverse-momentum and pseudorapidity distributions of charged hadrons in pp collisions at $\sqrt{s} = 0.9$ and 2.36 TeV", *JHEP* **02** (2010) 041, doi:10.1007/JHEP02(2010)041, arXiv:1002.0621.

[22] T. Sjöstrand et al., "An introduction to PYTHIA 8.2", *Comput. Phys. Commun.* **191** (2015) 159, doi:10.1016/j.cpc.2015.01.024, arXiv:1410.3012.

[23] CMS Collaboration, "Event generator tunes obtained from underlying event and multiparton scattering measurements", *Eur. Phys. J. C* **76** (2016) 155, doi:10.1140/epjc/s10052-016-3988-x, arXiv:1512.00815.

[24] I. P. Lokhtin and A. M. Snigirev, "A model of jet quenching in ultrarelativistic heavy ion collisions and high-p_{T} hadron spectra at RHIC", *Eur. Phys. J. C* **45** (2006) 211, doi:10.1140/epjc/s2005-02426-3, arXiv:hep-ph/0506189.

[25] D. J. Lange, "The EvtGen particle decay simulation package", *Nucl. Instrum. Meth. A* **462** (2001) 152, doi:10.1016/S0168-9002(01)00089-4.

[26] GEANT4 Collaboration, "GEANT4: a simulation toolkit", *Nucl. Instrum. Meth. A* **506** (2003) 250, doi:10.1016/S0168-9002(03)01368-8.

[27] M. L. Miller, K. Reygers, S. J. Sanders, and P. Steinberg, "Glauber Modeling in High Energy Nuclear Collisions", *Ann. Rev. Nucl. Part. Sci.* **57** (2007) 205, doi:10.1146/annurev.nucl.57.090506.123020, arXiv:nucl-ex/0701025.

[28] PHENIX Collaboration, "Detailed measurement of the e^+e^- pair continuum in $p+p$ and Au+Au collisions at $\sqrt{s_{\mathrm{NN}}}$ = 200 GeV and implications for direct photon production", *Phys. Rev. C* **81** (2010) 034911, doi:10.1103/PhysRevC.81.034911, arXiv:0912.0244.

[29] S. Plumari et al., "Charmed Hadrons from Coalescence plus Fragmentation in relativistic nucleus-nucleus collisions at RHIC and LHC", *Eur. Phys. J. C* **78** (2018) 348, doi:10.1140/epjc/s10052-018-5828-7, arXiv:1712.00730.

[30] Particle Data Group, M. Tanabashi et al., "Review of Particle Physics", *Phys. Rev. D* **98** (2018) 030001, doi:10.1103/PhysRevD.98.030001.

[31] CMS Collaboration, "Measurement of the $B^{\pm}$ meson nuclear modification factor in Pb-Pb collisions at $\sqrt{s_{\mathrm{NN}}}$ = 5.02 TeV", *Phys. Rev. Lett.* **119** (2017) 152301, doi:10.1103/PhysRevLett.119.152301, arXiv:1705.04727.

[32] CMS Collaboration, "CMS luminosity calibration for the pp reference run at $\sqrt{s} = 5.02$ TeV", CMS Physics Analysis Summary CMS-PAS-LUM-16-001, 2016.

[33] P. Skands, S. Carrazza, and J. Rojo, "Tuning PYTHIA 8.1: the Monash 2013 Tune", *Eur. Phys. J. C* **74** (2014) 3024, doi:10.1140/epjc/s10052-014-3024-y, arXiv:1404.5630.

[34] J. R. Christiansen and P. Z. Skands, "String Formation Beyond Leading Colour", *JHEP* **08** (2015) 003, doi:10.1007/JHEP08(2015)003, arXiv:1505.01681.

[35] M. He and R. Rapp, "Charm-Baryon Production in Proton-Proton Collisions", arXiv:1902.08889.